Supplementary material

Methods

Immunohistochemistry

The paraffin tissue blocks were sliced continuously to generate 4-μm thick slices, and the slices were heated at 65 °C for 1 h. The slides were then immersed in xylene for dewaxing and gradient alcohol for dehydration. Tris-EDTA buffer (pH 8.0) was added to the staining cylinder containing the slides. The samples were thereafter placed in the pressure cooker after boiling in water, and antigen repair was stopped for 3 min once the temperature increased to 120 °C. After natural cooling, endogenous peroxidase blocking solution was added, followed by 5% goat serum, and the membrane was incubated in a wet box at 4 °C overnight. The following primary antibodies were used: LPS (Hycult Biotech, 30443M1220), primary antibody LTA (Hycult Biotech, 30940M0321), CD33 (Boster Wuhan Dr. De, PB9932), Ly6C (Boster Wuhan Dr. De, A33313), and CD8 (LBP, R024). After rewarming, the tissue sections were incubated with goat anti-mouse and anti-rabbit IgG/IgM antibody (Abcam, ab2891) at 37 °C for 30 min, and the staining time was adjusted according to the staining depth (Gene Tech, GK3480). The slices were placed in distilled water to terminate color development for 1 min and then washed with tap water for 2 min. The sections were immersed in Mayer's hematoxylin staining solution and gently agitated for 30 s, followed by rinsing under running tap water for 10 min. After dehydration, the slides were mounted with neutral resin and examined by light microscopy. Images were captured, and immunohistochemical staining was quantitatively analyzed using ImageJ software[1,2].

Quantitative reverse transcription PCR

Total RNA was extracted using TRIzol reagent, and RNA concentration and purity were measured. After the removal of genomic DNA, a quantitative reverse transcription kit containing gDNA (Takara, Japan) was used for

reverse transcription and amplification. The sequences of the primers used for RT–qPCR are listed in Supplementary Table 2.

Cell lines

All human and murine cell lines were authenticated by short tandem repeat (STR) profiling and obtained from Shanghai Zhongqiao Xinzhou Biotechnology Co., Ltd. All cell lines used in this study are reported using their official nomenclature together with the corresponding Research Resource Identifiers (RRIDs), as curated in the ExPASy Cellosaurus database (e.g., MHCC-97H [RRID: CVCL_4972], LX-2 [RRID: CVCL_5792], HepG2 [RRID: CVCL_KS12], and Hepa1-6 [RRID: CVCL_0327]). All experiments were conducted using mycoplasma-free cell cultures.

Western blotting

After extracting protein from the tissue samples, the protein concentration was measured according to the instructions of the BCA protein concentration test kit (Beyotime, P0012). Subsequently, based on the measured total protein concentration, the required volumes of protein lysate and 5× loading buffer were calculated and mixed accordingly. The samples were then boiled at 100 °C for 10 min to ensure complete protein denaturation, briefly centrifuged for 10 s, and stored at −20 °C until further analysis. After mixing the gel and electrophoresis solution, electrophoresis was initiated. The concentration gel was exposed to 85 V for 30 min, and the separation gel was set at 100 V for 60 min. Electrophoresis was terminated when the bromophenol blue was approximately 1 cm away from the bottom. The membrane was transferred, and the transfer conditions included 286 mA of current for 2 h. Then, 5~10% skim milk was added to the membrane, which was placed on a shaker for 1 h after sealing. TBST was used to quickly wash the membrane 3 times on a shaker for 5 min each. The diluted primary antibody was added, and the samples were incubated at 4 °C overnight. The

membrane was quickly washed with TBST 3 times for 5 min each. The secondary antibody diluted with 5% skim milk was added to the membrane, which was incubated at room temperature for 1 h. TBST was used to thrice wash the membranes (5 min each time). The enhanced chemiluminescence (ECL) reagent was prepared according to the manufacturer's instructions and applied dropwise to the surface of the PVDF membrane. The exposure conditions were adjusted according to the different light intensities to ensure the quality of the images. Protein expression was quantified using ImageJ software.

$CD8^+$ T-cell proliferation experiment

C57BL/6 male mice aged 6–8 weeks were used for *in vivo* experiments. Following intragastric administration of CCl_4 for 4 weeks, 2×10^6 Hepa1-6 cells were orthotopically injected into the liver. Three weeks after tumor implantation, spleens were harvested from four tumor-bearing mice and immediately transferred into RPMI-1640 medium. In parallel, spleens were collected from four age-matched healthy C57BL/6 male mice and processed under identical conditions. Splenic single-cell suspensions were prepared and adjusted to a concentration of 1×10^8 cells/mL. $CD8^+$ T cells were isolated by magnetic bead–based positive selection according to the manufacturer's protocol (STEMCELL Technologies, Cat. No. 18953). Myeloid-derived suppressor cells (MDSCs) were isolated using magnetic bead–based negative selection in accordance with the manufacturer's instructions (STEMCELL Technologies, Cat. No. 19867). For carboxyfluorescein succinimidyl ester (CFSE) labeling, 3×10^6 $CD8^+$ T cells were incubated with 0.2 μL of 10 μM CFSE to achieve a final concentration of 2 μM. Cells were incubated at room temperature in the dark for 6 min, after which five volumes of RPMI-1640 medium supplemented with 10% fetal bovine serum (FBS) were added to terminate the reaction. The cells were further incubated for 2 min, followed by centrifugation at 450 × g for 5 min. After removal of the supernatant, cells

were washed twice with RPMI-1640 medium containing 10% FBS and resuspended in complete medium. CD3/CD28 antibodies (5 μg/3 μg) were diluted in 1 mL of phosphate-buffered saline (PBS), and 100 μL was added to each well, followed by incubation at 37 °C for 1 h. Subsequently, 1×10^5 CFSE-labeled $CD8^+$ T cells were seeded into antibody-coated wells and stimulated with recombinant interleukin-2 (IL-2; 50 U). MDSCs were added at $CD8^+$ T cell–to–MDSC ratios of 1:0.5 and 1:1, respectively, while $CD8^+$ T cells cultured in the absence of MDSCs served as controls. Co-cultures were maintained for 72 h. Following fixation, $CFSE^+$ $CD8^+$ T cells were collected by centrifugation and subjected to subsequent analyses.

Flow cytometry

HCC tissues were collected aseptically and placed into a centrifuge tube containing RPMI-1640. After grinding, digestion was performed with collagenase IV (Roche 0.5 mg/mL) and DNase I (Roche, 0.5 mg/mL). Following mechanical dissociation and filtration, single-cell suspensions were prepared from human hepatocellular carcinoma (HCC) tissues. Tumor-infiltrating mononuclear cells were subsequently isolated and stained using a human tumor-infiltrating tissue PBMC isolation kit (Solarbio, P3950), according to the manufacturer's instructions. For human samples, myeloid-derived suppressor cells (MDSCs) were identified using the following antibody panel: CD33 (PE), CD11b (PE-Cy7), and HLA-DR (APC). Detailed information for all flow cytometry antibodies is presented in Supplementary Table 3. Murine HCC tissues were processed into single-cell suspensions and subjected directly to antibody staining without prior PBMC isolation. Murine MDSCs were identified using the following antibody panel: CD45 (APC), CD11b (FITC), Ly6G (PerCP), and Ly6C (PE-Cy7). Following staining, cells were fixed with 500 μL of 4% paraformaldehyde at room temperature, resuspended in phosphate-buffered saline (PBS), and stored at 4 °C until acquisition. Prior to data acquisition, 200 μL of PBS was added, and

cell suspensions were passed through a 40-μm cell strainer before analysis on a BD FACSCanto™ II flow cytometer. Flow cytometry data were analyzed using FlowJo software.

Endotoxin assay

The abdomen was disinfected and opened using standard procedures. The tubes were arranged with sterile gauze soaked in saline. The anterior hepatic lobe was lifted to expose the portal vein. Blood was collected with sterile, heat-free insulin syringes. Serum was collected and diluted after centrifugation. An endotoxin test kit was used to measure the endotoxin concentration (Xiamen Limulus Reagent Biotechnology Company Limited, 32545s).

Fluorescence in situ hybridization (FISH)

The paraffin blocks were sectioned continuously at a thickness of 3 μm. A Cy3-labeled EUB338 FISH probe (Guangzhou Exon Biotechnology Company Limited, FB-0011B) was used. The EUB338 probe sequence was GCTGCCTCCCGTAGGAGT. The nonspecific probe non-EUB338 was used as the control, and the probe sequence was CGACGGAGGGCATCCTCA. Images were assessed using fluorescence microscopy according to the instructions of the EUB338 FISH Probe kit.

16S rDNA V3-V4 sequence

The CTAB/SDS method was used to extract total genomic DNA from the samples. The V3-V4 region of the 16S rDNA gene (515F-806R) was sequenced in 30 pairs of samples. Following the manufacturer's recommendations, sequencing libraries were generated using the NEBNext® Ultra™ IIDNA Library Prep kit (Cat No. E7645). Library quality was evaluated by a Qubit@ 2.0 fluorometer (Thermo Scientific) and an Agilent Bioanalyzer 2100 system. Finally, the library was sequenced on an Illumina NovaSeq platform, and

250-bp paired-end reads were generated. The DADA2 algorithm, implemented in QIIME2, was used for error modeling and filtering the raw fastq files. The absolute abundance rates of ASVs were normalized by rarefaction to a uniform sequencing depth corresponding to the sample with the lowest read count. All subsequent alpha-diversity and beta-diversity analyses were performed using the resulting normalized dataset.

Gating Strategy for Flow Cytometry Data

Flow cytometry data were analyzed using FlowJo software (TreeStar, USA). A hierarchical tree diagram of the detection markers was constructed based on the hierarchical relationships between markers[3]. Following established gating procedures, adherent cells and dead cells were excluded prior to data analysis, after which live single cells were selected for downstream gating. The Supplementary Figure 5 illustrate the gating strategy used to identify M-MDSCs and PMN-MDSCs in the tumor microenvironment of murine HCC tissues.

References

1 Fang Q, Zheng S, Chen Q, Chen L, Yang Y, Wang Y, Zhang H, Chen J. The protective effect of inhibiting mitochondrial fission on the juvenile rat brain following PTZ kindling through inhibiting the BCL2L13/LC3 mitophagy pathway. *Metab Brain Dis* 2023; **38**: 453-466 [PMID: 36094724 DOI: 10.1007/s11011-022-01077-3]

2 Varghese F, Bukhari AB, Malhotra R, De A. IHC Profiler: an open source plugin for the quantitative evaluation and automated scoring of immunohistochemistry images of human tissue samples. *PLoS One* 2014; **9**: e96801 [PMID: 24802416 DOI: 10.1371/journal.pone.0096801]

3 Zhao H, Zhou Y, Xu J, Zhang Y, Wang H, Zhao C, Huang H, Yang J, Huang C, Li Y, Wang L, Nie Y. Short-chain fatty acid-producing bacterial strains attenuate experimental ulcerative colitis by promoting M2

macrophage polarization via JAK/STAT3/FOXO3 axis inactivation. *J Transl Med* 2024; **22**: 369 [PMID: 38637862 DOI: 10.1186/s12967-024-05122-w]

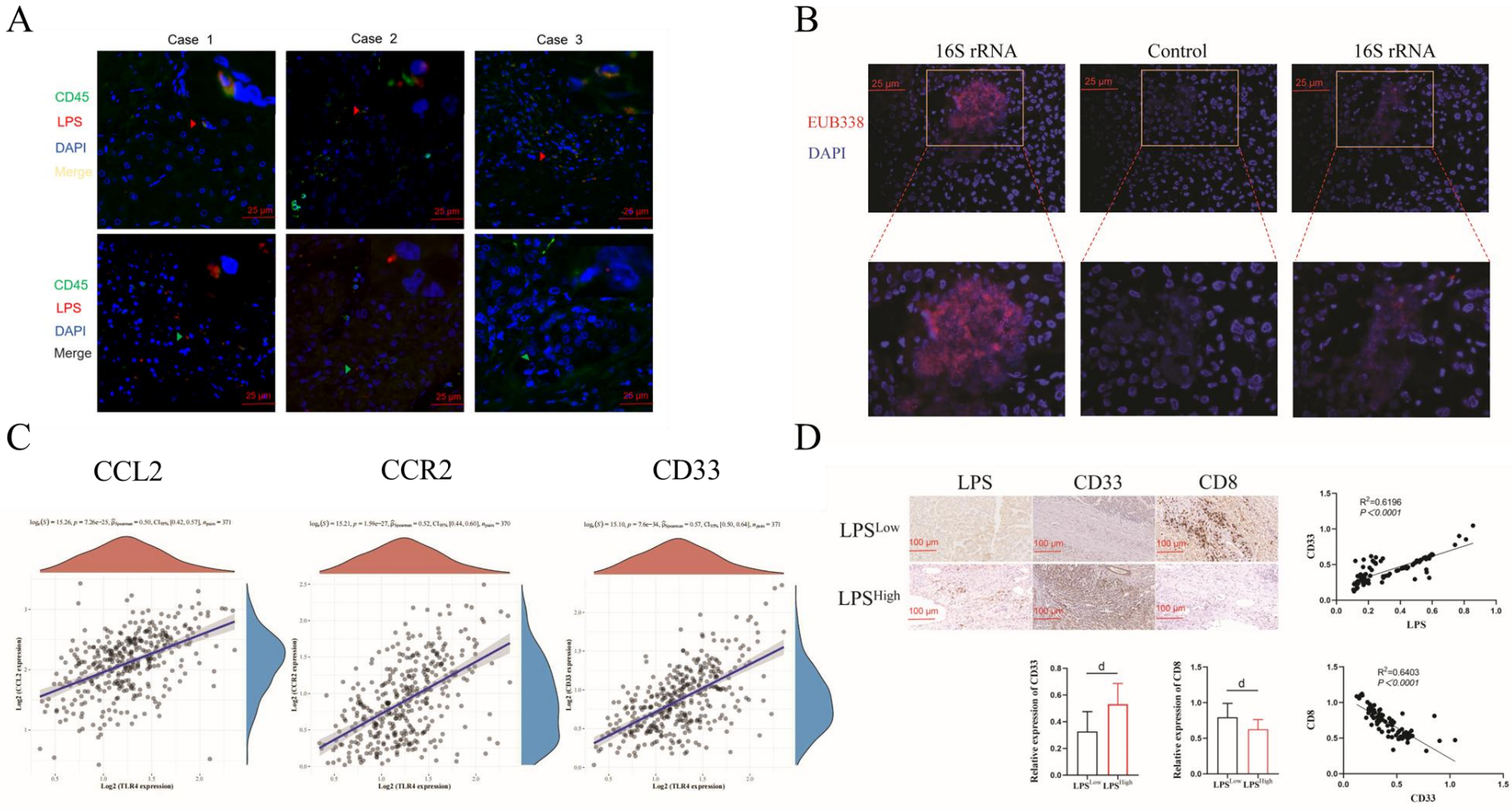
A
Case 1
Case 2
Case 3
CD45
LPS
DAPI
Merge
25 μm
B
16S rRNA
Control
16S rRNA
EUB338
DAPI
C
CCL2
CCR2
CD33
Log2 (CCL2 expression)
Log2 (CCR2 expression)
Log2 (CD33 expression)
Log2 (TLR4 expression)
D
LPS
CD33
CD8
LPSLow
LPSHigh
100 μm
R2=0.6196
P <0.0001
R2=0.6403
P <0.0001
Relative expression of CD33
Relative expression of CD8
d

Supplementary Figure 1 There were differences in lipopolysaccharide^{low} and lipopolysaccharide^{high} in hepatocellular carcinoma. A: Lipopolysaccharide (LPS) was present alongside immune nuclei (shown in red triangle) and non-immune nuclei (shown in green triangle) by LPS and CD45 immunofluorescence co-localization; B: Bacterial 16S rRNA was also found in the same region and located near the nucleus by continuous pathological sections; C: The correlations between TLR4 and CCL2, TLR4 and CCR2, TLR4 and CD33 genes; D: The correlations between of LPS and CD33; The correlations between of CD33 and CD8 (LPS^{low} n = 47, LPS^{high} n = 46, $^{d}P < 0.0001$).

A

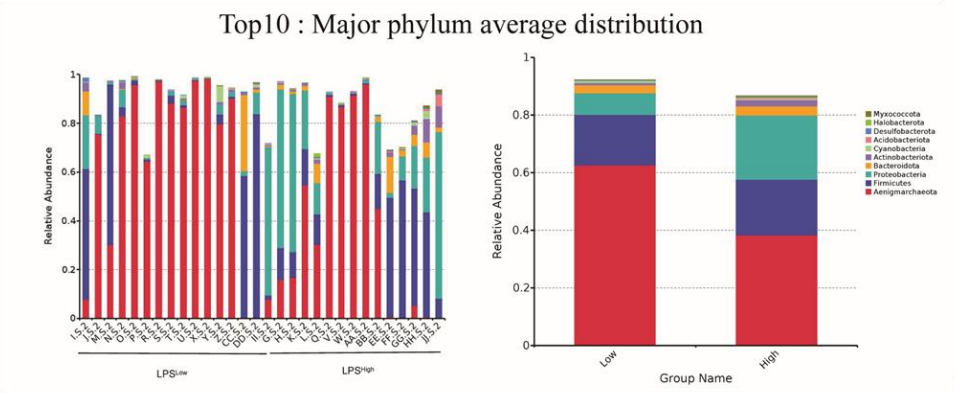
Top10 : Major phylum average distribution
Relative Abundance
Group Name
Low
High
Myxococcota
Halobacterota
Desulfobacterota
Acidobacteriota
Cyanobacteria
Actinobacteriota
Bacteroidota
Proteobacteria
Firmicutes
Aenigmarchaeota

B

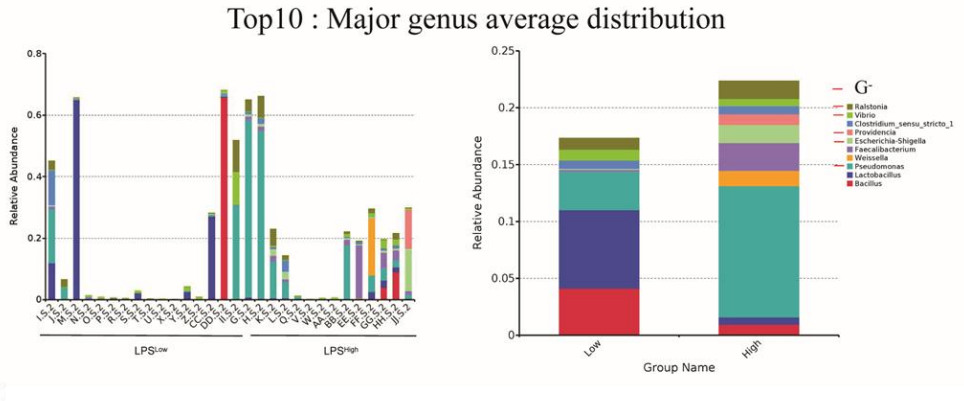
Top10 : Major genus average distribution
Relative Abundance
Group Name
Low
High
G-
Ralstonia
Vibrio
Clostridium_sensu_stricto_1
Providencia
Escherichia-Shigella
Faecalibacterium
Weissella
Pseudomonas
Lactobacillus
Bacillus

C

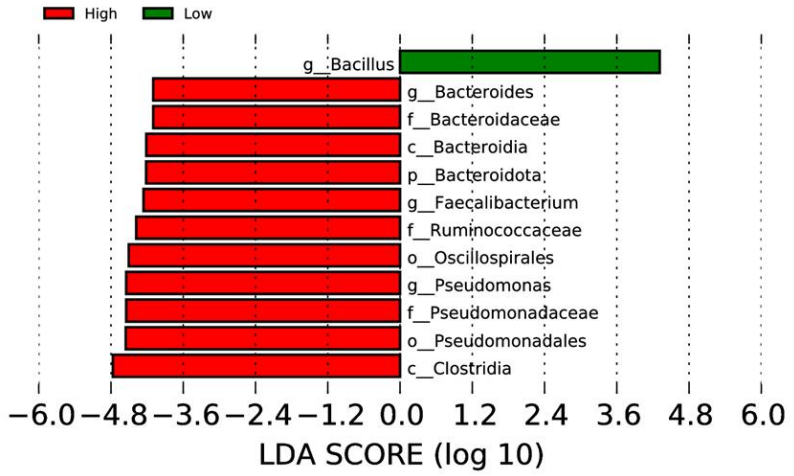
High
Low
g__Bacillus
g__Bacteroides
f__Bacteroidaceae
c__Bacteroidia
p__Bacteroidota
g__Faecalibacterium
f__Ruminococcaceae
o__Oscillospirales
g__Pseudomonas
f__Pseudomonadaceae
o__Pseudomonadales
c__Clostridia
−6.0 −4.8 −3.6 −2.4 −1.2 0.0 1.2 2.4 3.6 4.8 6.0
LDA SCORE (log 10)

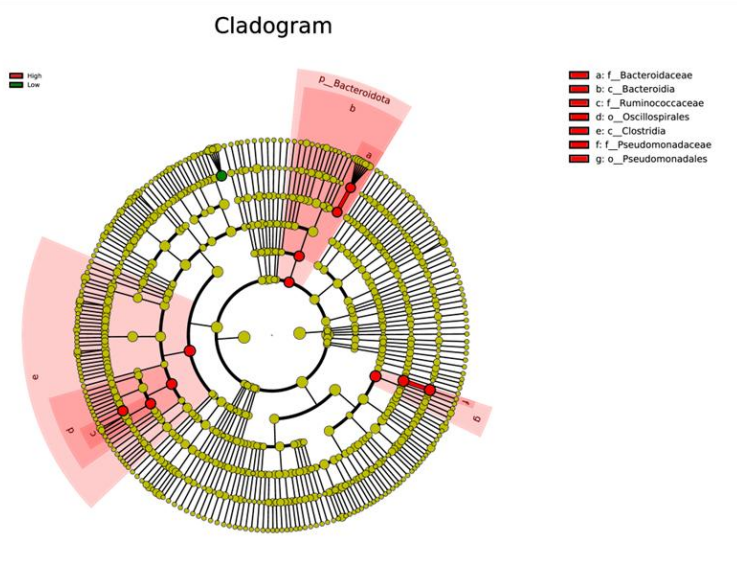
Cladogram
a: f__Bacteroidaceae
b: c__Bacteroidia
c: f__Ruminococcaceae
d: o__Oscillospirales
e: c__Clostridia
f: f__Pseudomonadaceae
g: o__Pseudomonadales
p__Bacteroidota

Supplementary Figure 2 The microflora composition of lipopolysaccharide^{high} group was different from that of lipopolysaccharide^{low} group. A: Major phylum average distribution in LPS^{Low} and LPS^{High} groups; B: Major genus average distribution in LPS^{Low} and LPS^{High} groups; C: The LDA bar distribution plot and evolutionary cladogram from LEfSe analysis in LPS^{Low} and LPS^{High} groups (LPS^{Low} n = 16, LPS^{High} *n* = 14).

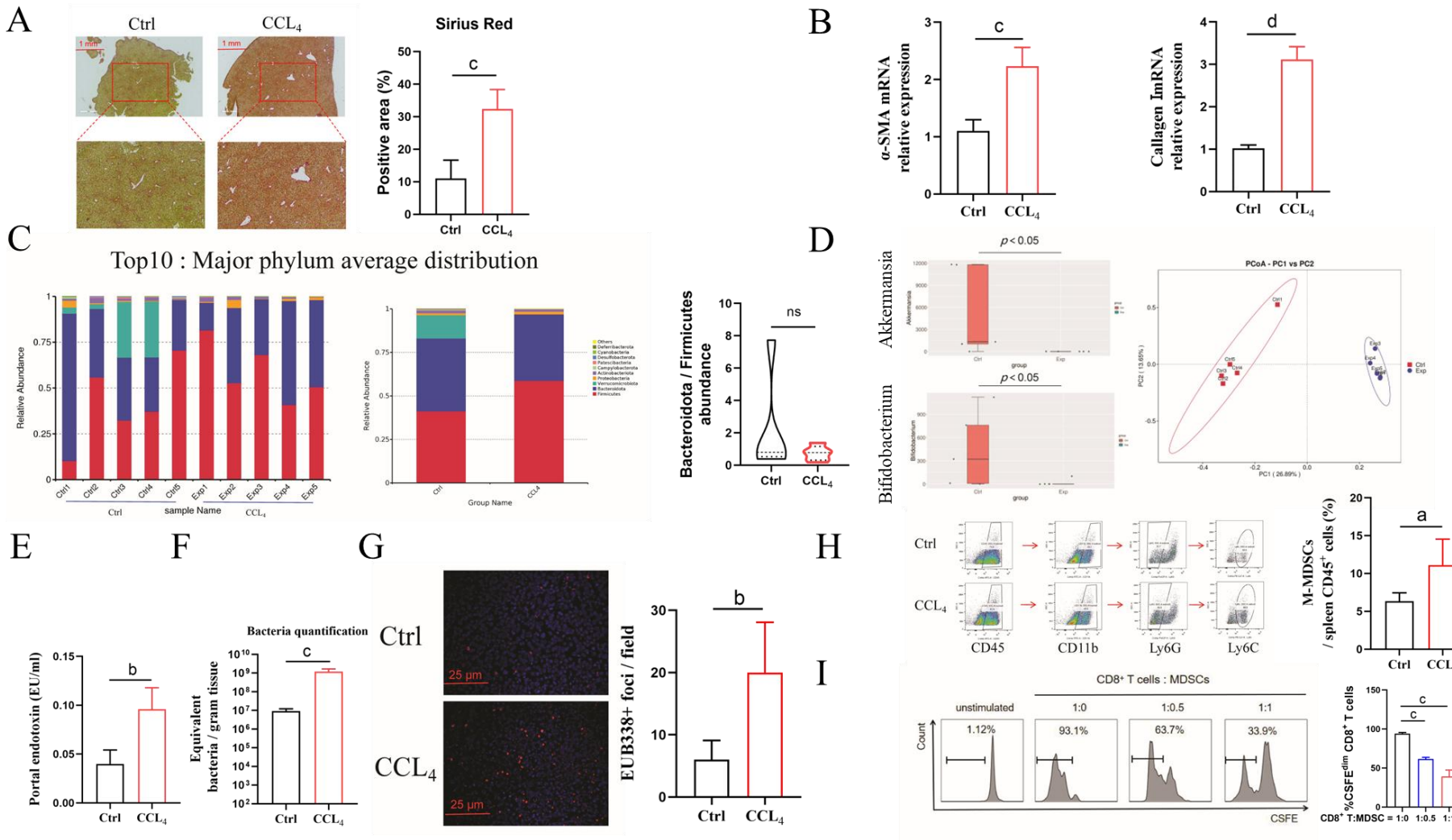
A
Ctrl
CCL4
1 mm
Sirius Red
Positive area (%)
c
Ctrl
CCL4
B
α-SMA mRNA relative expression
c
Ctrl
CCL4
Callagen ImRNA relative expression
d
Ctrl
CCL4
C
Top10 : Major phylum average distribution
Relative Abundance
Ctrl1
Ctrl2
Ctrl3
Ctrl4
Ctrl5
Exp1
Exp2
Exp3
Exp4
Exp5
Ctrl
sample Name
CCL4
Group Name
Others
Deferribacterota
Cyanobacteria
Desulfobacterota
Patescibacteria
Campylobacterota
Actinobacteriota
Proteobacteria
Verrucomicrobiota
Bacteroidota
Firmicutes
Bacteroidota / Firmicutes abundance
ns
Ctrl
CCL4
D
Akkermansia
Bifidobacterium
p < 0.05
p < 0.05
group
PCoA - PC1 vs PC2
PC1 (26.89%)
PC2 (13.65%)
Ctrl
Exp
E
Portal endotoxin (EU/ml)
b
Ctrl
CCL4
F
Bacteria quantification
Equivalent bacteria / gram tissue
c
Ctrl
CCL4
G
Ctrl
CCL4
25 μm
25 μm
EUB338+ foci / field
b
Ctrl
CCL4
H
Ctrl
CCL4
CD45
CD11b
Ly6G
Ly6C
M-MDSCs / spleen CD45+ cells (%)
a
Ctrl
CCL4
I
CD8+ T cells : MDSCs
unstimulated
1:0
1:0.5
1:1
1.12%
93.1%
63.7%
33.9%
Count
CSFE
%CSFEdim CD8+ T cells
c
c
CD8+ T:MDSC = 1:0
1:0.5
1:1

Supplementary Figure 3 Impaired intestinal mucosal barrier exposes the liver to the gut microbiota. A: The positive area of Sirius red in CCL_4 group was higher than that in Ctrl group; B: The relative mRNA expression levels of α smooth muscle actin and Callagan I in the CCL_4 group were higher than those in Ctrl group; C: Major phylum average distribution in the Ctrl and CCL_4 groups. The ratio of Bacteroidetes/Firmicutes in Ctrl and CCL_4 groups; D: The bacterial abundance rates of *Akkermansia* and *Bifidobacterium* in CCL_4 group were lower than those in the Ctrl group. Principal coordinate analysis using weighted-UniFrad of beta diversity indicated a different distribution of Ctrl and CCL_4 groups; E: The level of portal endotoxin in CCL_4 group was higher than that in Ctrl group; F: The presence of bacterial DNA in hepatocellular carcinoma tissues was assessed by quantitative PCR targeting bacterial 16S rDNA. The bacterial DNA expression levels of CCL_4 group was higher than that of Ctrl group; G: The change of bacterial 16S rRNA in Ctrl and CCL_4 group; H: Gating strategies of the flow cytometric data of monocytic myeloid-derived suppressor cells in spleen of Ctrl and CCL_4 groups (n = 5 for each group); I: Inhibition of $CD8^+$ T cell proliferation by myeloid cells was assessed by flow cytometry of $CD8^+$ T cells in co-culture experiments. $^aP < 0.05$, $^bP < 0.01$; $^cP < 0.001$; $^dP < 0.0001$.

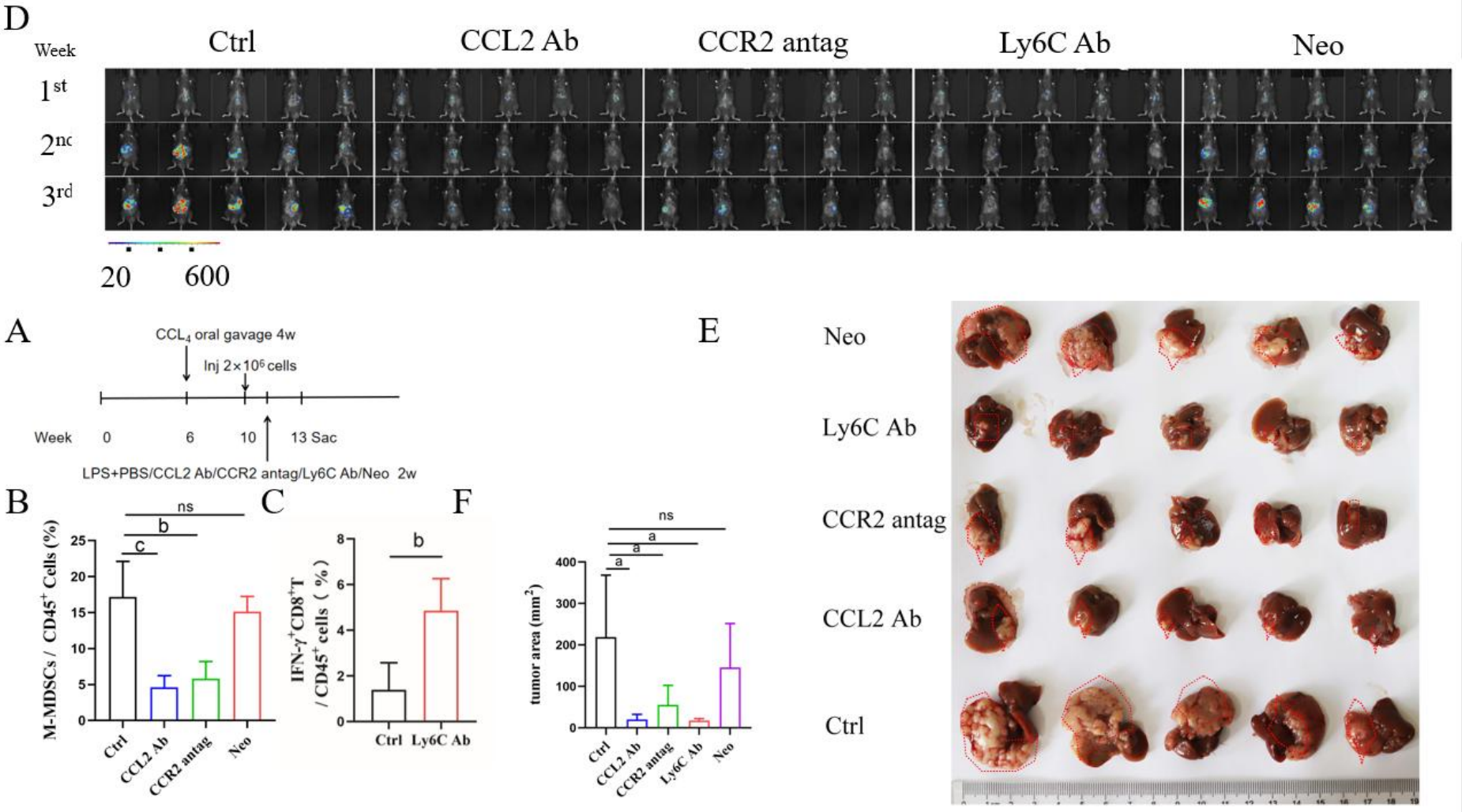
D
Week
Ctrl
CCL2 Ab
CCR2 antag
Ly6C Ab
Neo
1st
2nd
3rd
20
600
A
CCL4 oral gavage 4w
Inj 2×10^6 cells
Week 0 6 10 13 Sac
LPS+PBS/CCL2 Ab/CCR2 antag/Ly6C Ab/Neo 2w
B
M-MDSCs / CD45+ Cells (%)
ns
b
c
Ctrl
CCL2 Ab
CCR2 antag
Neo
C
IFN-γ+CD8+T / CD45+ cells (%)
b
Ctrl
Ly6C Ab
F
tumor area (mm2)
ns
a
a
a
Ctrl
CCL2 Ab
CCR2 antag
Ly6C Ab
Neo
E
Neo
Ly6C Ab
CCR2 antag
CCL2 Ab
Ctrl

Supplementary Figure 4 Targeting CCL2/CCR2/monocytic myeloid-derived suppressor cell under exogenous lipopolysaccharide reduced the effect of LPS on hepatocellular carcinoma and inhibited tumor growth. A and E: Schematic illustration of the animal intervention protocol and experimental outcomes; B: Accumulation of monocytic myeloid-derived suppressor cells (MMDSCs) in tumor tissues was quantified by flow cytometry in the Ctrl, CCL2 Ab, CCR2 antag, and neomycin groups; C: Infiltration of interferon-γ-positive $CD8^+$ T cells (IFN-γ^+ $CD8^+$ T cells) was assessed in the Ctrl and Ly6C Ab groups; D: Tumor growth was monitored by weekly *in vivo* imaging in the control (Ctrl), CCL2 antibody (CCL2 Ab), CCR2 antagonist (CCR2 antag), Ly6C antibody (Ly6C Ab), and neomycin treatment groups; F: Changes in tumor size were evaluated in the Ctrl, CCL2 Ab, CCR2 antag, Ly6C Ab, and neomycin groups. n = 5 mice per group). $^aP < 0.05$, $^bP < 0.01$; $^cP < 0.001$; $^dP < 0.0001$.

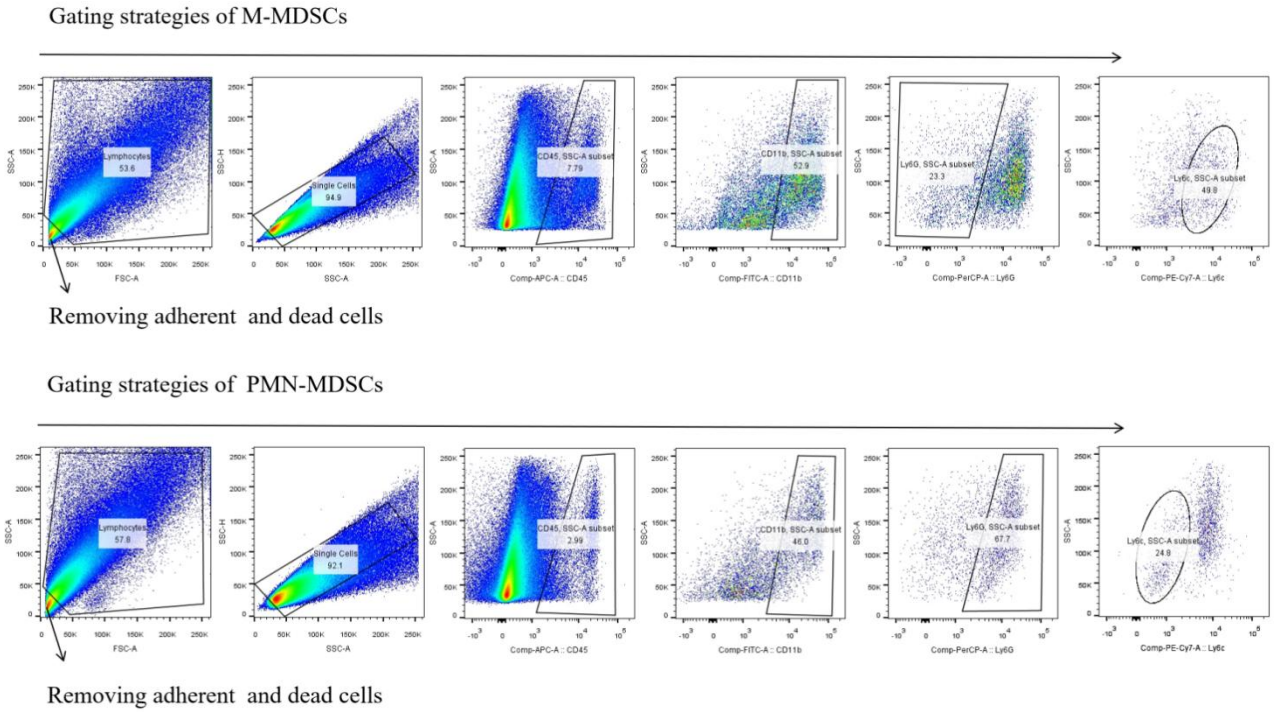

Supplementary Figure 5 Gating strategies of the flow cytometric data of monocytic myeloid-derived suppressor cells and polymorphonuclear-myeloid-derived suppressor cells.

Supplementary Table 1 List of clinical characteristics for 14 validation hepatocellular carcinoma cohort

Characteristic		Cases
LPS^{Low}		8
LPS^{High}		6
Age	Median	53 (year old)
Gender	Female	5
	Male	9
Grade	I-II	5
	III-IV	9
TNM Stage	I-II	6
	III-IV	8

Supplementary Table 2 Bacterial strain in hepatocellular carcinoma tissues were detected List using selective culture plates

Bacterial	Sample solution	LPS^{Low}	LPS^{High}	Gram stain
Klebsiella pneumoniae	-	-	+	G-
Stenotrophomonas maltophilia	-	-	+	G-
Haemophilus parainfluenzae	-	-	+	G-
Acinetobacter guillouiae	-	-	+	G-
Staphylococcus aureus	-	+	-	G+
Staphylococcus capitis	-	+	-	G+

Supplementary Table 3 Primer sequence

Primer	Forward Primer (5′ to 3′)	Reverse Primer (5′ to 3′)
m (Collangen Ⅰ)	CCTCAGGGTATTGCTGGACAAC	CAGAAGGACCTTGTTTGCCAGG

m (α-SMA)	CTCTGTCTGGATCGGTGGC	TTCGTCGTATTCCTGTTTGCT
m (IL-1β)	AGAGCATCCAGCTTCAAATCTC	CAGTTGTCTAATGGGAACGTCA
m (IL-17A)	CAGACTACCTCAACCGTTCCAC	TCCAGCTTTCCCTCCGCATTGA
m (GAPDH)	CATCACTGCCACCCAGAAGACTG	ATGCCAGTGAGCTTCCCGTTCAG
m(TLR4)	AGCTTCTCCAATTTTTCAGAACTTC	TGAGAGGTGGTGTAAGCCATGC
m(CCL2)	GCTACAAGAGGATCACCAGCAG	GTCTGGACCCATTCCTTCTTGG
m(CCR2)	GCTGTGTTTGCCTCTCTACCAG	CAAGTAGAGGCAGGATCAGGCT
m(Ly6C)	GCGCCTCTGATGGATTCTGCAT	ATCCCTGATTGGCACACCAGCA
h(TLR4)	CCCTGAGGCATTTAGGCAGCTA	AGGTAGAGAGGTGGCTTAGGCT
H(GAPDH)	GTCTCCTCTGACTTCAACAGCG	ACCACCCTGTTGCTGTAGCCAA
h(CCL2)	AGAATCACCAGCAGCAAGTGTCC	TCCTGAACCCACTTCTGCTTGG

Supplementary Table 4 Flow cytometry antibodies information

Name	Supplier and Article number
APC anti-human HLA-DR	Biolegend, 980406
PE anti-human CD33	Biolegend, 983904
PE-Cyanine7 anti-human CD11b	Biolegend, 982608
FITC anti-mouse CD11b	Biolegend, 101205
APC anti-mouse/human CD11b	Biolegend, 101211
PerCP anti-mouse Ly6G	Biolegend, 127654
PE-Cyanine7 anti-mouse Ly6C	BD Biosciences, 560593
PE-Cyanine7 anti-mouse Gr-1	BD Biosciences, 557598
Brilliant Violet 605 anti-mouse CD3	BD Biosciences, 564009
Intracellular staining perm wash buffer	Biolegend, 421002
FITC anti-mouse CD8a	Biolegend, 162313
APC anti-mouse CD45	Biolegend, 157605
PE-Cyanine7 anti-mouse CD8a	Biolegend, 100721
PE anti-mouse IFN-γ	Biolegend, 505807
PE anti-mouse CCR2	Biolegend,150609